www.czasopisma.pan.pl PAN www.journals.pan.pl

ARCHIVES of FOUNDRY ENGINEERING

ISSN (2299-2944)
Volume 18
Issue 2/2018

151 – 156

DOI: 10.24425/122519

27/2

Published quarterly as the organ of the Foundry Commission of the Polish Academy of Sciences

Evaluating the Attenuation in Ultrasonic Testing of Castings

M. Boháčik *, M. Mičian, A. Sládek
Department of Technological Engineering, University of Zilina, Univerzitna 1, 010 26 Zilina, Slovakia
* Corresponding author. E-mail address: michal.bohacik@fstroj.uniza.sk

Received 06.03.2018; accepted in revised form 08.06.2018

Abstract

This paper considers the assessment of attenuation in aluminium alloys castings and in cast iron prepared by gravity casting method and by casting under pressure. The issue of ultrasound attenuation is important in setting the conditions of non-destructive (NDT) testing, especially in casted materials. The characteristics of the ultrasonic technique and ultrasonic attenuation and the calculation of the attenuation and the velocity of ultrasound are presented in the theoretical part of this paper. For experimental measurements, cylindrical castings from AlSi alloy (a hypoeutectic alloy with a silicon content of about 7% - AlSi7 and a eutectic alloy with a silicon content of about 12% - AlSi12) and from grey and ductile cast iron were made. The ultrasonic records of the casting control, the calculation of ultrasound attenuation for individual samples are listed and described in the experimental part. The evaluation of measurements and comparison of calculated ultrasound attenuation is at the end of this article.

Keywords: AlSi alloy, Cast Iron, Technological casting parameters, Ultrasound attenuation

1. Introduction

Ultrasonic testing has arisen from the need to detect internal defects of forgings and rollers where cannot be used X-Ray testing and where these defects could cause serious damage of machine parts. The ultrasonic inspection of all casted materials are not as widespread as the inspection of other construction materials. The biggest problem with ultrasound testing is in the coarse anisotropic grain structure on which the ultrasonic beam is scattered, as the material has different mechanical and physical properties in each direction. Problematic ultrasound inspection of castings is also due to the fact, that during casting production volume errors which are spatially indented and randomly oriented often occur [3, 4]. Several factors influence the outcome of the ultrasound test such as device, probe, acoustic bond, the test surface, material, the shape of the test part, and so on. In graphitic cast iron is attenuation of the ultrasound caused also by the graphite shape and dispersion in the matrix of the base material. Some castings can be tested with 5 MHz probes, but in some cases, 3.5 MHz or 2 MHz probes are needed. For larger sizes of castings, probes with a lower frequency than 2 MHz are needed. After heat treatment, ultrasonic attenuation is often reduced. [4, 6]

2. Attenuation of ultrasound

As the ultrasound wave suddenly passes through the environment, its acoustic pressure decreases and thus its energy, resulting in a growing distance from the source due to the expansion of the ultrasound waves to a still increasing environment. The reason for this decline is the attenuation due to absorption and ultrasound scattering. Absorption occurs because of internal friction of oscillating particles, plastic flow, relaxation and thermal phenomena. The mechanical energy of oscillating particles is transformed into thermal energy. With increasing frequency, absorption losses also increase. They are strongly dependent on temperature [2, 5]. With an ideal planar wave where there is no scattering on the sides, the sound pressure with increasing distance from the source would not change (but that would only be in the case of an ideal and homogeneous material). In real conditions, the sound pressure drop with the distance is always bigger. It has two main causes [2, 9]:

- scattering of waves at microscopic interfaces (e.g., grain structures),
- absorption of waves (energy absorption by internal friction of vibrating particles).

The dispersion of ultrasonic waves occurs in non-homogeneous and polycrystalline environment, whether solid or liquid. During the impact of ultrasound on individual inhomogeneities at their interface, there is reflection, refraction and bending, because the acoustic impedance changes on each interface. In solids, these are mainly small groups of inhomogeneities such as inclusions, graphite bodies, pores or grains of metal and cast materials. These inhomogeneities are mostly randomly oriented and therefore the ultrasound wave disperses into all directions. The bending of the ultrasonic waves depends on the size of the inhomogeneities and the frequency, and therefore the dispersion of the ultra-sound varies according to the dimension of the inhomogeneities and the wavelength. During the wave dispersion, the ultrasound energy does not change to another kind of energy, but disappears from the directed ultrasonic field. The structure of solids is usually inhomogeneous [1, 4, 7]. The total ultrasound attenuation at a given thickness is expressed by factor α and has a unit of dB/mm. It is given by the sum of individual losses [2]:

$$\alpha = \alpha_P + \alpha_R \quad [\mathrm{dB/mm}] \tag{1}$$

where:
- α_P is the loss by material absorption [dB/mm],
- α_R is the loss by scattering ultrasound wave [dB/mm].

$$\alpha = \frac{\Delta dB}{2h} = \frac{A}{2h} \quad [\mathrm{dB/mm}] \tag{2}$$

where:
- ΔdB is the level of dB,
- h is height of cylindrical sample [dB/mm].

$$A = 20 \cdot \log \frac{P_0}{P} \approx 20 \cdot \log \frac{H_0}{H} \quad [\mathrm{dB}] \tag{3}$$

where:
- A is the level of dB,
- P_0, P are the amplitudes of the reference acoustic pressures [Pa],
- H_0, H are the heights of the compared echoes on the UT device screen [%].

The total attenuation equals the sum of the ultrasound trajectory and the coefficient of attenuation α. In a reflection method where the wave passes a double path, the total attenuation is calculated from the relationship [2, 4]:

$$u = 2 \cdot d \cdot \alpha \tag{4}$$

where:
- u is the total attenuation [dB],
- d is the thickness of the material [mm],
- α is the coefficient of attenuation [dB/mm].

The absorption attenuation of the transverse waves at the same wavelength is lower than in the longitudinal waves. The attenuation by absorption is caused by internal friction and elastic hysteresis (at higher frequencies) and is there-fore directly proportional to the frequency. At higher frequencies, the attenuation coefficient is mostly determined by scattering. In general, if the size of inhomogeneties and anisotropy of crystals is increasing, the scatter losses are also increasing. The greatest influence on the scatter losses has the relationship between the wavelength λ and the mean size of inhomogeneties D. Losses caused by scattering tend to be higher in transverse waves than in longitudinal waves. Therefore, the overall attenuation of the transverse waves is larger at the same wavelength than in the longitudinal waves. As mentioned in the introduction, the biggest problem with ultrasound testing is in the coarse anisotropic grain structure on which the ultrasonic beam is scattered. In Fig. 1 you can see an example of anisotropic material, where the good direction of testing and direction with big attenuation is shown. [2 - 4]

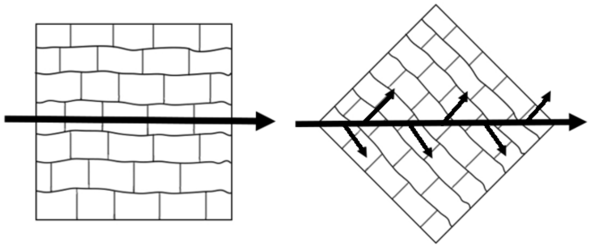

Fig. 1. Testing of anisotropic material – good direction of testing (left), direction with big attenuation (right) [2]

A lower frequency should be chosen for the testing of materials with a coarse structure or non-homogeneous materials such as concrete, ceramics, rocks, wood and grey cast iron. In addition, plastics have a big attenuation, so they only leak lower frequencies. Fine grain ceramics, brass, bronze, some rocks and some types of alloys have the medium attenuation. The lowest loss can be expected for fine-grained steel, aluminium and magnesium. There is a great difference between the attenuation of metallic material with a moulded or cast structure.

Materials with cast structure, such as the various types of castings, exhibit a large grain, and therefore their attenuation tends to be higher. The scattering on the grains of the material structure is dependent on the ratio of the wavelength to the mean grain size. The longer the wavelength approaches the size of the grains, the bigger attenuation there is. [4, 8]

3. Attenuation testing of test samples

In the experimental part, the results for two types of Al-Si aluminium alloys are presented. A hypoeutectic alloy with a silicon content about 7% (AlSi7) and a eutectic alloy with a silicon content about 12% (AlSi12) were used. After the experimental measurements for evaluated materials, next step was also to evaluate attenuation for samples made of grey (GJL) and ductile cast iron (GJS).

Eutectic alloys are distinguished by their excellent fluidity. Therefore, they are used for complex castings, thin-walled castings, mainly in the automotive and aerospace industries. They are frequently used in pressure and chillmold casting. From the AlSi12 alloy, thin-walled and complex castings are produced, such as motor covers, switchgear cabinets, pump components, and gauge cases.

Preparation for melting and casting of samples was carried out in the laboratory of casting at the Department of Technological Engineering at University of Zilina.

AlSi type alloys were prepared from a primary alloy which already contained an inoculant and a modifier. The test samples from AlSi aluminium alloy were cast by a direct casting method with crystallisation under pressure and gravitationally. A manual hydraulic press ASTA A-20005, whose maximum thrust load is 20 tonnes, was used to apply the pressure. When designing the mold, it was necessary to take into account the dimensions of the equipment, the future shape of the casting and its easy removal, as well as the simplest possible manufacturing process. For these reasons, a cylindrical ingot mold was designed where the cavity was conical in shape. The melting of the aluminium alloy was carried out in electrical resistance furnace in a graphite crucible threated with a protective refractory material. After melting to the appropriate casting temperature, the molten alloy was poured into the pre-heated mold with dimensions of Ø 35 x 50mm using the ladle. The samples, from both types of alloy, were cast gravitationally and under pressure using piston of hydraulic press, until it was not casting solidification of samples completed (about 45 seconds). Subsequently, all test samples were machined into dimensions of Ø 30 x 43mm.

For the preparation of cast iron, crude iron, steel scrap, litvar7 type modifier and graphitization inoculant FeSi75 were used. Experimental samples were casted into steel molds with dimensions Ø 55-150mm. The steel molds were put into another mold made from sand. This san mold was compacted by hand. The inflow system had the intake on the bottom of the mold. Casting was provided into two molds at once. One mold contained a cooler and the other a riser. Later casting was provided into the mold containing only coolers for the purpose of creating a crust in the area where the cooler met the molted cast iron. After this there was an assumption that a shrinkage will be created inside of the sample. Experimental samples were created from grey cast iron (GJL) and ductile cast iron (GJS). Then samples were machined to achieve the desired dimensions (Ø50-140 mm) and surface quality.

The individual technological parameters casting of the test samples are shown in Table 1 and Table 2.

Table 1.
Technological parameters of the test samples casting of aluminium alloys

Sample number	Material	The casting temperature [°C] (± 5°C)	Mold temperature [°C] (± 5°C)	Pressure [MPa]
1	AlSi7	735	250	Casted gravitationally
2	AlSi7	735	250	30
3	AlSi12	700	150	Casted gravitationally
4	AlSi12	700	200	150

Table 2.
Technological parameters of the test samples casting of cast iron

Sample number	Material	The casting temperature [°C] (± 5°C)	Pressure [MPa]
5	GJL	1450	Casted gravitationally
6	GJS	1500	Casted gravitationally

The length of the sample has been chosen so that the sample can be reliably tested by ultrasound. Individual samples were then subjected to evaluate ultrasound attenuation. The OmniScan MX2 modular defectoscope from Olympus was used for testing. The measurement was performed from the forehead of the test samples in three places. Two probes with the label were used:

- C126 5MHz/0.375″
- A550S-SM 3.5MHz/0.375″

At sample No. 1 (AlSi7), it was not possible to capture the reflected echo. It was captured only a weak end-effect echo with significant noise (valid for the 3.5MHz and 5MHz probes), therefore, it was not possible to determine the attenuation. The ultrasound record from this measurement is shown in Fig. 2. Other samples were well evaluable, it was captured the end echo and the first reflected echo, so we could evaluate the magnitude of the attenuation. An example of a measurement record on sample No. 1 and No. 2 is shown in Fig. 2 and in Fig. 3. In Tab. 3 and in Tab. 4, the results of attenuation for AlSi7 material are shown. The axes of figures 2-5 are described below Fig. 5.

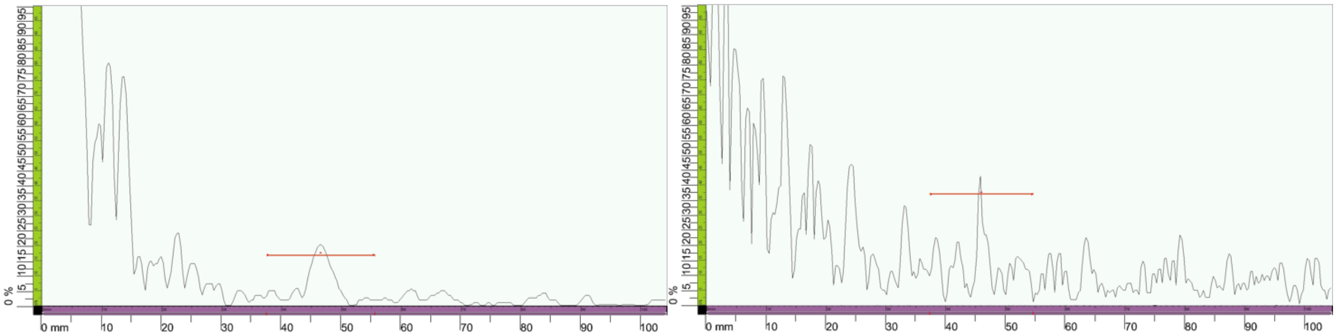

Fig. 2. Recording of evaluating attenuation of sample No. 1 (left – 3.5 MHz probe, right - 5 MHz probe frequency)

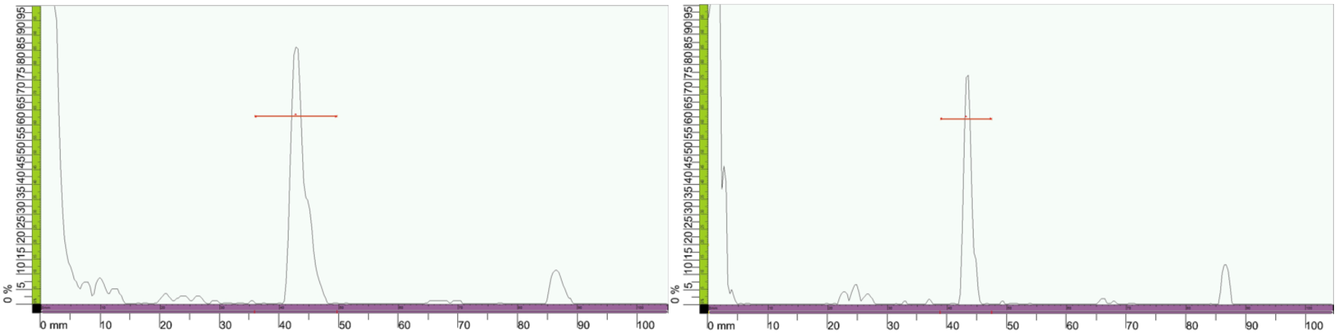

Fig. 3. Recording of evaluating attenuation of sample No. 2 (left – 3.5 MHz probe, right - 5 MHz probe frequency)

Table 3.
Ultrasonic attenuation values for AlSi7 test samples (3.5 MHz probe frequency)

Sample number/measurement number	H_0 [%]	H [%]	h [mm]	c_L [m. s^{-1}]	α [dB.mm^{-1}]	Average of α [dB.mm^{-1}]
1	not measured	not measured	43	not evaluated	not evaluated	-
2/1	86	11	43		0,208	
2/2	75	8	43	6580,0	0,226	0,227
2/3	82	7	43		0,249	

where:
α is the coefficient of attenuation [dB/mm],
c_L is velocity of the longitudinal ultrasonic wave [m. s^{-1}],
h is height of cylindrical sample [dB/mm],
H_0, H are the heights of the compared echoes on the UT device screen [%].

Table 4.
Ultrasonic attenuation values for AlSi7 test samples (5 MHz probe frequency)

Sample number/measurement number	H_0 [%]	H [%]	h [mm]	c_L [m. s^{-1}]	α [dB.mm^{-1}]	Average of α [dB.mm^{-1}]
1	not measured	not measured	43	not evaluated	not evaluated	-
2/1	76	14	43		0,178	
2/2	86	12	43	6542,6	0,199	0,225
2/3	83	4,3	43		0,299	

Test samples from AlSi12 alloys in all samples were able to capture the end echo and reflected echo, so we could determine the ultrasound attenuation. An example of a measurement record on sample No. 3 is shown in Fig. 4. In Tab. 5 and Tab. 6, the results of the evaluation of attenuation for AlSi12 material are shown.

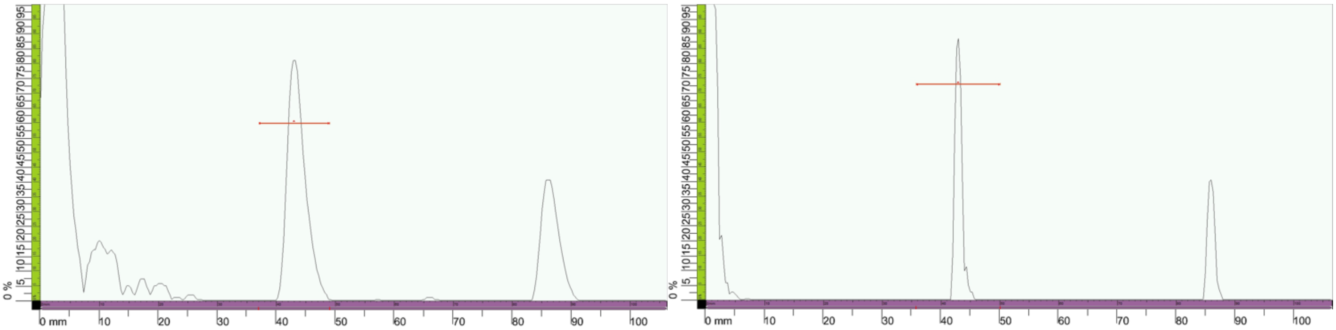

Fig. 4. Recording of evaluating attenuation of sample No. 3 (left – 3.5 MHz probe, right - 5 MHz probe frequency)

Table 5.
Ultrasonic attenuation values for AlSi12 test samples (3.5 MHz probe frequency)

Sample number/measure ment number	H_0 [%]	H [%]	h [mm]	c_L [m. s^{-1}]	α [dB.mm^{-1}]	Average of α [dB.mm^{-1}]
3/1	81	41	43		0,069	
3/2	80	24	43	6646,1	0,121	0,107
3/3	84	23	43		0,130	
4/1	81	24	43		0,123	
4/2	80	26	43	6542,6	0,113	0,105
4/3	96	44	43		0,079	

Table 6.
Ultrasonic attenuation values for AlSi12 test samples (5 MHz probe frequency)

Sample number/measure ment number	H_0 [%]	H [%]	h [mm]	c_L [m. s^{-1}]	α [dB.mm^{-1}]	Average of α [dB.mm^{-1}]
3/1	89	41	43		0,078	
3/2	84	38	43	6661,5	0,080	0,095
3/3	81	24	43		0,123	
4/1	77	32	43		0,089	
4/2	89	39	43	6504,9	0,084	0,091
4/3	89	33	43		0,100	

Test samples from cast irons alloys in all samples were able to capture the end echo and reflected echo, so we could determine the ultrasound attenuation. An example of a measurement record on sample No. 5 and No. 6 is shown in Fig. 5. In Tab. 7, the results of the evaluation of attenuation for cast iron material are shown.

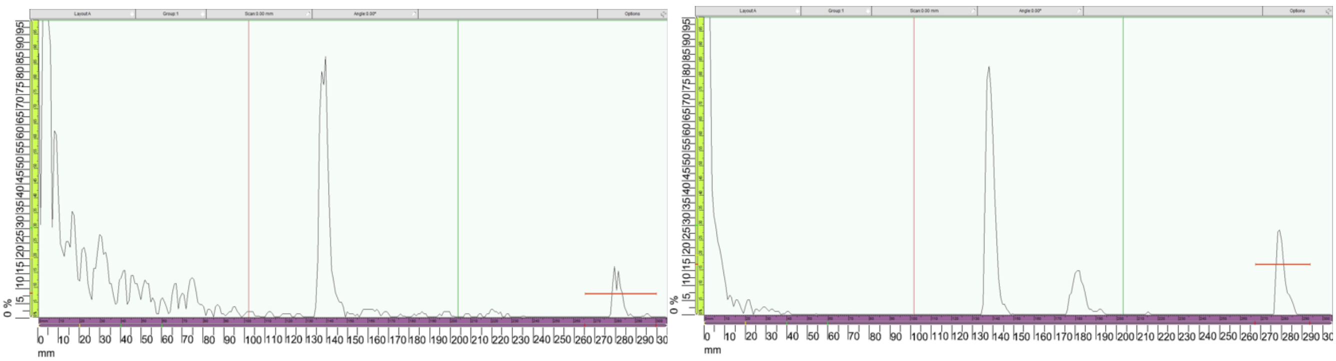

Fig. 5. Recording of evaluating attenuation of sample No. 5 (left) and No. 6 (right) - 3.5 MHz probe frequency

where:

Axe x is Range of the time base [mm],
Axe y is Full screen height [%].

Table 7.
Ultrasonic attenuation values for cast iron test samples (3,5 MHz probe frequency)

Sample number/ measurement number	A_0 [%]	A_1 [%]	h [mm]	c_L [m. s^{-1}]	α [dB.mm^{-1}]	Average of α [dB.mm^{-1}]
5/1	82	41	140		0,022	
5/2	80	25	140	4658,9	0,036	0,033
5/3	86	22	140		0,042	
6/1	87	23	140		0,041	
6/2	79	21	140	5768,4	0,041	0,034
6/3	85	45	140		0,020	

4. Conclusions

The coefficient of attenuation in the casting inspection significantly influences the applicability of ultrasonic tech-niques to assess internal errors. Cast materials, compared to formed alloys, have bigger attenuation considering the nature of the internal structure. The presented paper shows the results of the attenuation for two variants of aluminium alloy based on AlSi and two types of cast iron. The material was casted with a variety of technological parameters (different mold temperatures and aplied pressure – for aluminium alloys). Some samples were also cast gravitationally. The effect of these parameters should influence the resulting structure of the casting, which would have an effect on ultrasound attenuation.

The results show that in material AlSi7 casted gravitationally we could not measure out end-effect echo, so we could not be able to determine the attenuation. For the casting under pressure we measured the average attenuation 0.227 dB.mm^{-1} (when using a 3.5 MHz probe) and 0.225 dB.mm^{-1} (when using a 5 MHz probe). For the AlSi12 type alloy, the change in attenuation was mainly due to the change in applied pressure. With increasing pressure attenuation decreased, respectively there was the difference between gravity casting and casting under the pressure (sample No. 3 and No. 4). With the increase of the mold temperature in this type of alloy, the value of the attenuation (sample No. 4) has decreased. Generally, the increased pressure would have to temper the grain size, while slower cooling (raising the mold temperature) tends to increase the susceptibility to grain growth. The results also point to the fact that the hypoeutectic Al-Si alloy results in greater attenuation than the same type of alloy with the eutectic composition. All of these conclusions point to the significant influence of casting method and chemical composition of aluminium alloy. The use of ultrasonic techniques to evaluate the internal defects of castings from this type of material, must be considered with these regularities. While casting samples from cast iron, the higher attenuation was reached in test samples from ductile cast iron. The difference in attenuation between grey and ductile cast iron was minimal.

Until now, we have not done microstructure yet, so the impact of the attenuation on the structure type could not be evaluated yet. Only the impact of attenuation on technological parameters such as casting temperature, aluminum alloy type, and type of graphite in cast iron were evaluated. For that, in the next stages of research from the presented area, the objective will be to produce microstructural samples and suitably describe them structurally and search for the magnitude of the ultrasound attenuation from the individual parameters of test samples microstructure. The goal in aluminium alloys will be to evaluate sdas factor and in cast iron to determine length of graphite precipitates.

References

[1] Aweda, J.O., Adeyemi, M.B. (2012). Experimental Determination of Heat Transfer Coefficients During Squeeze Casting of Aluminium. An Overview of Heat Transfer Phenomena. Dr M. Salim Newaz Kazi (Ed.). ISBN 978-953-51-0827-6. InTech. DOI: 10.5772/52038.

[2] Boháčik, M., Mičian, M. & Koňár, R. (2017). Evaluating the attenuation in ultrasonic testing for AlSi alloys castings. *Manufacturing Technology: Journal for Science, Research and Production*. 17(5), 669-674. ISSN 1213-2489.

[3] Boháčik, M., Mičian, M., Koňár, R. & Hlavatý, I. (2017). Ultrasonic testing of butt weld joint by TOFD technique. *Manufacturing Technology*. 17(6), 842-847. ISSN 1213-2489.

[4] Konar, R., Patek, M. & Zrak, A. (2015). Ultrasonic testing of non-ferrous materials in the foundry industry. *Manufacturing Technology*. 15(4), 557-562. ISSN 1213-2489.

[5] Lehocká, D., Hlavatý, I. & Hloch, S. (2016). Rationalization of Material Flow in Production of Semitrailer Frame for Automotive Industry. *Tehnicki Vjesnik-Technical Gazette*. 23(4), 1215-1220.

[6] Vasková, I., Hrubovčáková, M., Malik, J. & Eperješi, Š. (2014). Influence of technological parameters of furane-mixtures on shrinkage creation in ductile cast iron castings. *Archives of Metallurgy and Materials*. 59(3), 1037-1040. DOI: 10.2478/amm-2014-0174.

[7] Lee, J.H., Kim, H.S., Won, C.W. & Cantor, B. (2002). Effect of the gap distance on the cooling behavior and the microstructure of indirect squeeze cast and gravity die cast 5083 wrought Al alloy. *Materials Science & Engineering A*. 338(1-2), 182-190. Elsevier.

[8] Gucwa, M., Winczek, J., Bęczkowski, R. & Dośpiał, M. (2016). Structure and properties of coatings made with self-shielded cored wire. *Archives of Foundry Engineering*. 16(3), 39-42.

[9] Bruna, M., Bolibruchova, D. & Pastircak, R. (2017). Reoxidation Processes Prediction in Gating System by Numerical Simulation for Aluminium Alloys. *Archives of Foundry Engineering*. 17(3), 23-26.